

Study of Exact and High-Frequency Code Solvers for Applications to a Conformal Dipole Array

S. D. Walker and D. Chatterjee

Department of Computer Science and Electrical Engineering
University of Missouri-Kansas City (UMKC), Kansas City, MO 64110, USA
chatd@umkc.edu

(Invited Paper)

Abstract – The embedded element pattern of a conformal dipole array of seven elements is calculated using integral equation algorithms in exact solvers such as FEKO and WIPL-D, with the central element excited and other elements match-terminated in a 50Ω load. A technique is developed that uses the FEKO subdomain basis function current weights to derive the equivalent current weight for a single entire domain basis function for use in the high-frequency code NECBSC. This process includes effects of mutual coupling in the NECBSC calculations. The results for the embedded element pattern for cylinders with $ka = 10, 20, 30, 40, 60$ and 80 , computed via FEKO, WIPL-D, and NECBSC, reveal discrepancies in the deep shadow (or creeping wave) regions. Parametric simulation studies for dipole currents, by varying the cylinder radius or radial distance of the array arc from the cylinder curved surface, are also included.

I. Introduction

Conformal arrays, flush-mounted on electrically large convex bodies, often cannot be analyzed by *exact* numerical techniques due to increased demands for computational resources [1]. The integral equation (EFIE) methods [2], [3] require a discretization size of $\lambda/10$ for such electrically large structures, where λ is the wavelength. This presents a practical difficulty in using exact solvers such as WIPL-D [4] and FEKO [5] that solve the radiation/scattering problem by discretization of the EFIE. In contrast, the *Uniform Theory of Diffraction* (UTD) [3], [6] is particularly suitable for electrically large problems because it does not require structural discretization at any frequency. The subject of this investigation is the calculation of element patterns of a single ring, sectoral dipole array in presence of an

electrically large PEC cylinder shown in Fig. 1.

The UTD formulations in the NECBSC code require antennas to be 0.25λ off the cylinder curved surface [7]. With reference to Fig. 1, a cylindrical dipole array was studied in [8] which serves as a motivation for the work reported here. The high-frequency radiation from such an array in the shadow ($\phi \rightarrow 180^\circ$ in Fig. 1) regions can be described in terms of “*creeping waves*”. Past investigations on creeping wave radiation have shown discrepancies between exact and UTD results [9]-[11] for isolated single sources located off the cylinder curved surface. However, these studies did not consider conformal array [8] radiation, and hence are distinct from the present investigation. A methodology to accomplish this comparative analysis for conformal arrays, by combining appropriate solutions from both exact [5] and high-frequency code [7] solvers, is the purpose of this investigation.

The results in this paper are restricted to a 7-element dipole array because such a model retains all the canonical features without unnecessarily complicating the problem. Validation studies of the exact code solvers available in [12]-[14] lent confidence in their application to conformal array problems. Finally, this paper is an extension of but is mostly distinct from [15].

The conformal array problem and its NECBSC solution is described in the next section. This is followed by extensive results and their discussion. The conclusions are summarized with a list of relevant references.

II. Problem Description and Solution Methodology

For an array with large number of elements the

total array element pattern in the radiation zone is generically written as:

$$F(r, \theta, \phi) = \frac{e^{-jkr}}{r} g_{elm}(\theta, \phi) \sum_{n=1}^N C_n e^{j\psi_n} \quad (1)$$

The summation in (1) indicates the (complex) array factor of N elements with complex (current or voltage) excitations C_n ; ψ_n is the phase at n^{th} element. The $g_{elm}(\theta, \phi)$ is the embedded element pattern of a single element while all other elements are terminated in a matched load. The $g_{elm}(\theta, \phi)$ varies across a finite array because the elements close to the array edges “see” a different environment than the ones at the center. It is implicit that $g_{elm}(\theta, \phi)$ contains the effects of the mutual coupling from nearby elements. The exact solvers in [4], [5] can directly calculate the array mutual coupling unlike [7]. Thus, a method by which array mutual coupling can be included in NECBSC output is the main contribution of this paper.

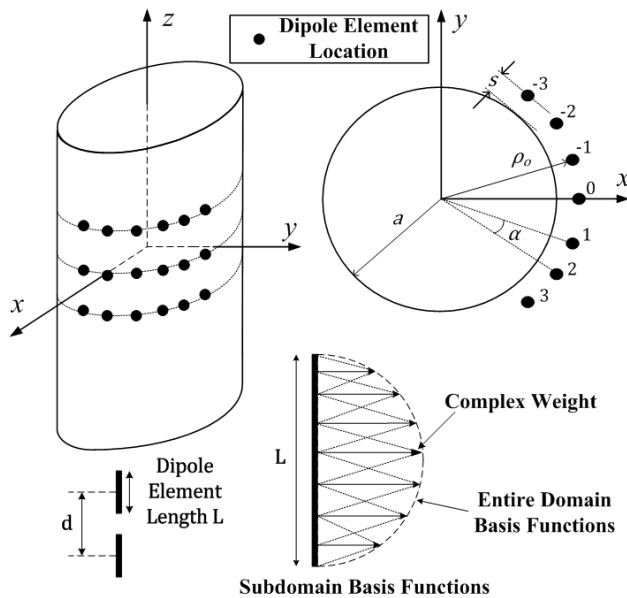


Fig. 1. Geometry of a conformal cylindrical dipole array of $\lambda/2$ dipole; the cylinder radius is ka and the dipoles have an inter-arc spacing of b/λ , and are off the PEC curved surface of the cylinder by a distance s/λ . In the present problem, only a single arc-ring, 7-element, azimuthally located dipole array is considered. Here $b = \alpha\rho_0$ with $\rho_0 = a + s$. The numbering scheme for the 7-element array is also shown.

To that end, the analysis developed gainfully utilizes FEKO output currents which include mutual coupling effects *in-situ*. The FEKO uses overlapping triangular basis function on the individual dipole elements. If the current on the dipole element is $i(z)$, it can be expressed in the two forms as,

$$i(z) = \begin{cases} \sum_{p=1}^P \Psi_{\Delta}(z) I_{\Delta}^p, & \text{for FEKO} \\ I_0 \cos\left(\frac{\pi z}{L}\right), & \text{for NECBSC} \end{cases} \quad (2)$$

The dipole of length L is discretized into P segments in FEKO and over each segment the overlapping triangular basis functions with weights I_{Δ}^p are used. In the NECBSC a purely entire domain basis function can be used [7]. For the NECBSC, $-L/2 \leq z \leq L/2$; in the FEKO code, the triangular basis function in (2) is given as:

$$\Psi_{\Delta}(z) = \begin{cases} \frac{z - z_{p-1}}{z_p - z_{p-1}}, & \text{for } z_{p-1} \leq z \leq z_p \\ \frac{z_{p+1} - z}{z_{p+1} - z_p}, & \text{for } z_p \leq z \leq z_{p+1} \end{cases} \quad (3)$$

The I_{Δ}^p are the *complex* current weights associated with the triangular basis functions in FEKO. These can be directly obtained in the output file of FEKO through use of appropriate input commands to store these segment currents, when developing the input geometry file. Our objective is to express I_0 in terms of the FEKO segment currents I_{Δ}^p . From (2) and (3) it readily follows that

$$I_0 \int_{-L/2}^{L/2} \cos^2\left(\frac{\pi z}{L}\right) dz = \sum_{p=1}^P I_{\Delta}^p \int_{-L/2}^{L/2} \Psi_{\Delta}(z) \cos\left(\frac{\pi z}{L}\right) dz \quad (4)$$

Further reduction of (4) then produces the desired result,

$$I_0 = \frac{4}{\pi} \left[\frac{\sin^2\left(\frac{\pi \Delta L}{4L}\right)}{\frac{\pi \Delta L}{4L}} \right] \sum_{p=1}^P I_{\Delta}^p \sin\left(\frac{\pi z_p}{L}\right) \quad (5)$$

In (5) $\Delta L = z_{p+1} - z_{p-1}$. The node at z_p falls midway between the $(p+1)^{th}$ and $(p-1)^{th}$ nodes. The complex current weight I_{Δ}^p is associated with the location of the p^{th} node. It is reiterated that I_0 in (5) is a complex current weight. To summarize, (5) allows a very convenient way of incorporating the mutual coupling information in the NECBSC code from a-priori information of the same from the FEKO code.

III. Results and Discussion

The results are shown in Figs. 2 to 15. The numerical data are shown in the figure captions therein. For the FEKO calculations, dipoles of length $L = \lambda/2$ were discretized into $P = 51$ to 101 segments, which yields the node location $z_p = p(L/P)$, with $p = 1, 2, 3, \dots, P$. For either 51 or 101 segments on the dipole, the corresponding equivalent complex current weight I_0 from (5) was found not to be significantly different. The results are discussed briefly below. In Figs. 2 and 3 magnitude and phase comparisons between I_0 obtained via (5), and the I_{Δ}^p on the central segment of the excited (#0) dipole is shown for increasing s/λ . The comparison reveals the two features:

- I_{Δ}^p on the central segment of the dipole, as available from the FEKO output file, is a very good approximation to I_0 obtained via (5). This is expected because I_0 is the maxima at the center of the support region of the cosinusoidal entire domain basis function.
- The decaying oscillatory nature of the magnitude and phase with s/λ . This is due to the standing wave interactions between the dipole and the cylinder curved surface. As the dipole array moves away from the cylinder curved surface, the degree of this interaction decreases and is evidenced by the decrease in the peaks and nulls in the variations.

Figures 4 and 5 show the effects of the scattering structure, which is the electrical radius ka of the cylinder, on the current I_0 using (5). The I_0 data in these figures were computed for each of the individual seven elements in the dipole array from the corresponding FEKO output file.

The dominant effect of the cylinder radius ka on the current magnitudes is noticeable on the central (excited) element as in Fig. 4. The current magnitude I_0 on the farthest elements (#2, -2, 3 &

-3) in Fig. 4 is apparently insensitive to increase in ka . However the same figure shows that the noticeable influence of the cylinder curvature on the excited (or central #0) element for $ka = 10 \rightarrow 50$. Beyond $ka \geq 50$, the curvature effects are imperceptible.

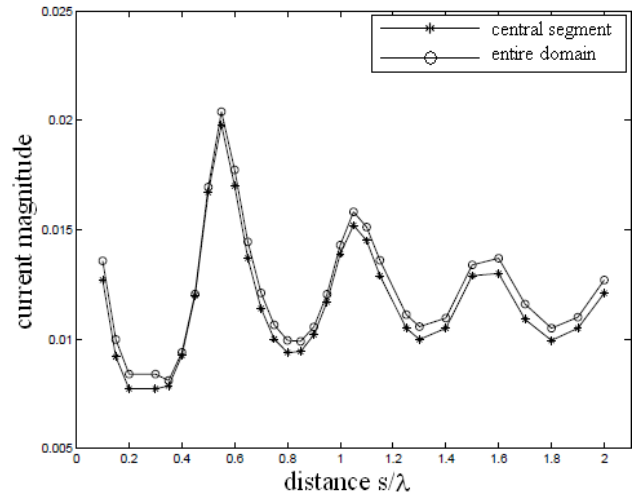


Fig. 2. Current amplitude variation on the excited dipole (#0) element located at the array center; $ka = 30$, $b/\lambda = 0.5$, $L/\lambda = 0.5$ and the cylinder height is $H/\lambda = 10$. All other dipoles are terminated in a 50Ω load. The entire domain result refers to (5).

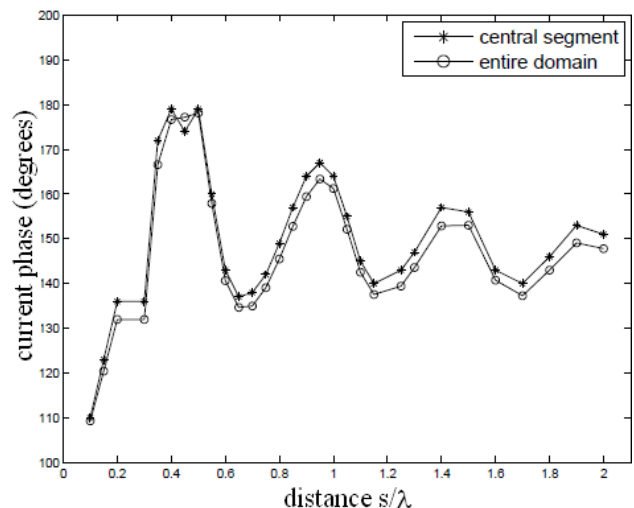


Fig. 3. Current phase variation on the excited dipole (#0) element located at the array center; $ka = 30$, $b/\lambda = 0.5$, $L/\lambda = 0.5$ and the cylinder height is $H/\lambda = 10$. All other dipoles are terminated in a 50Ω load. The entire domain result refers to (5).

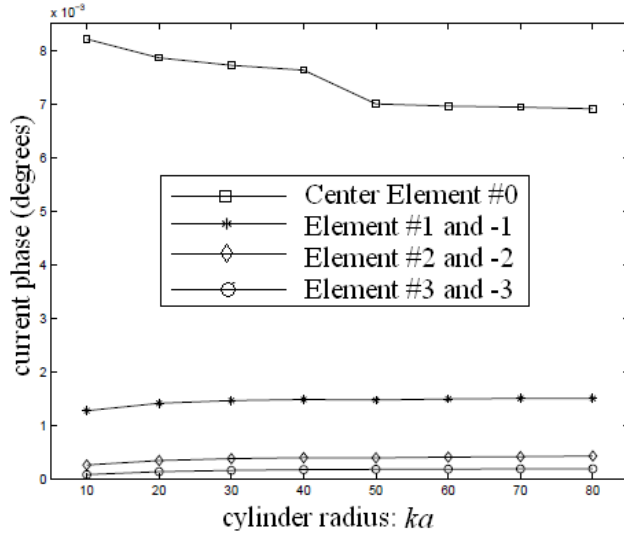


Fig. 4. Current magnitude variation on all the dipole elements; $b/\lambda = 0.5$, $L/\lambda = 0.5$, $s/\lambda = 0.25$ and the cylinder height is $H/\lambda = 10$. The central dipole element (#0) is excited, with all others terminated in a 50Ω load. The entire domain result refers to (5).

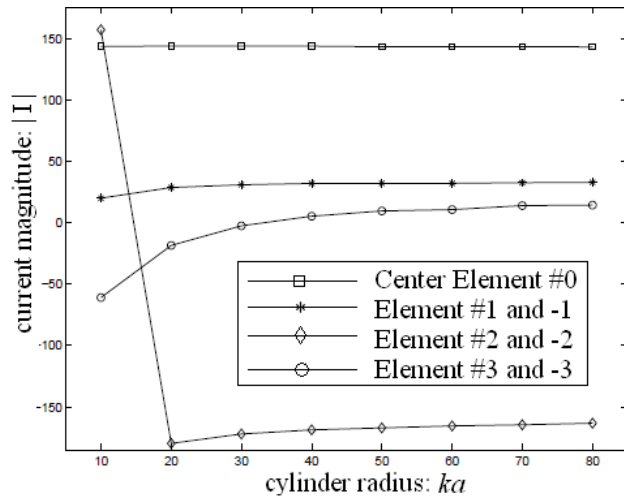


Fig. 5. Current phase variation on all the dipole elements; $b/\lambda = 0.5$, $L/\lambda = 0.5$, $s/\lambda = 0.25$ and the cylinder height is $H/\lambda = 10$. The central dipole element (#0) is excited, with all others terminated in a 50Ω load. The entire domain result refers to (5).

A similar conclusion can be arrived by examining the sensitivity of the phase of the currents on the individual dipole elements in Fig. 5. (The single point at $ka = 10$ for element #2 and -2, appears to be an exception, and is apparently intractable at this stage.) While there is a marked difference in the levels, the increase of cylinder radius apparently causes little change in the element phases.

The results in Figs. 4 and 5 present some interesting and useful insights into computation involving electrically large conformal arrays. The information gleaned suggests that because the current I_0 is relatively insensitive to increase in cylinder radius ka , it may be reasonable to obtain these currents for an electrically small cylinder using exact code solvers (FEKO or WIPL-D) and then subsequently use them to calculate scattering by an electrically large cylinder using high-frequency solvers like the NECBSC code. This process would result in substantial savings in computational resources. Based on the results presented here, it appears that the embedded element pattern, $g_{elm}(\theta, \phi)$, would not be substantially different obtained by this proposed approach.

Figures 6 to 15 show the azimuth ($\theta = 90^\circ$) plane embedded element pattern for the central dipole (#0) with others terminated in a matched load, and, for a wide range of cylinder radius ($ka = 10$ to 80). All other data is included in the figures and is omitted here. For the NECBSC results, the excitation currents for every individual element in the dipole array were computed via equation (5). This implies that the NECBSC results include mutual coupling effects when the center dipole is excited.

The results in Figs. 6 to 9 generally exhibit similar nature. For $ka = 10$ and 20 the differences between FEKO, WIPL-D and NECBSC in the shadow (creeping wave) region is not significant. However the same is not generally true for the results in Figs. 10 to 12.

The results in Figs. 8 and 9 are explained in some detail here. The NECBSC result in Fig. 9 was obtained by using the FEKO current weight on the central segment of each dipole element in the array. In contrast in Fig. 8, the currents for NECBSC data was obtained via (5). The comparison of the NECBSC embedded element pattern, $g_{elm}(\theta, \phi)$, suggests that there is only minimal variation in the embedded element pattern and it is noticeable in the deep shadow regions only.

The comparative analysis of the embedded element patterns for electrically large cylinders is shown in Figs. 10 to 12. The results indicate good agreement in the 'lit' region - where the geometric optics ray fields exist - for cylinders of electrical radius $ka = 40$ (Fig. 10). All the three cases show marked disagreements in the creeping wave or deep

shadow regions. Interestingly, in Figs. 11 ($ka = 60$) and 12 ($ka = 80$), the differences in the results from the exact and high-frequency code solvers are also noticeable in the lit regions.

The effects of varying s/λ on the embedded element pattern is shown in Figs. 13 to 15. Including the result in Fig. 8, imparts a broader overview. The results indicate that the increase of s/λ is somewhat unpredictable. For example, the result in Fig. 13 shows the worst agreement between the three codes. However this trend is not predictive as the distance s/λ is increased to 0.75 (Fig. 14) and 1.0 (Fig. 15). In the latter two figures the level of disagreement is less pronounced in the deep-shadow or creeping wave regions as compared to the corresponding one in Fig. 13. Note that in Fig. 8 the disagreement is less compared to Fig. 13.

The results indicate that NECBSC scattering formulations in the creeping wave region of PEC convex surfaces need more theoretical investigations. This was also observed in earlier investigations [9] and [10]. In both these cases the high-frequency fields in the creeping wave region of a PEC elliptic and circular cylinders were found to disagree with the exact analysis for the same problem. The numerical results for the embedded element pattern for investigation presented here appears to confirm the earlier conclusions in [9] and [10] for a similar (but not identical) problem.

Finally, our results are at variance with the earlier investigations in [11]. The analysis in [11] was specifically for a line source. In particular, this present study did not investigate in detail the effects decreasing s/λ height as was done in [11]. The minimum height chosen was $s/\lambda = 0.25$ for the results in this paper, while in [11] the UTD curved surface scattering formulations were studied for very small heights $s/\lambda = 0.05$. The choice of the minimum height in this paper specifically focused on examining the limits of applicability of the NECBSC code, and not necessarily the general UTD formulations.

To that end, it appears instructive following the results and conclusions in [11] to examine the effects of the height factor in view of the more recent work in [6]. The various high-frequency formulations and their regions of validity has been studied there, and its application to conformal dipole arrays such as in [8] needs to be more carefully investigated.

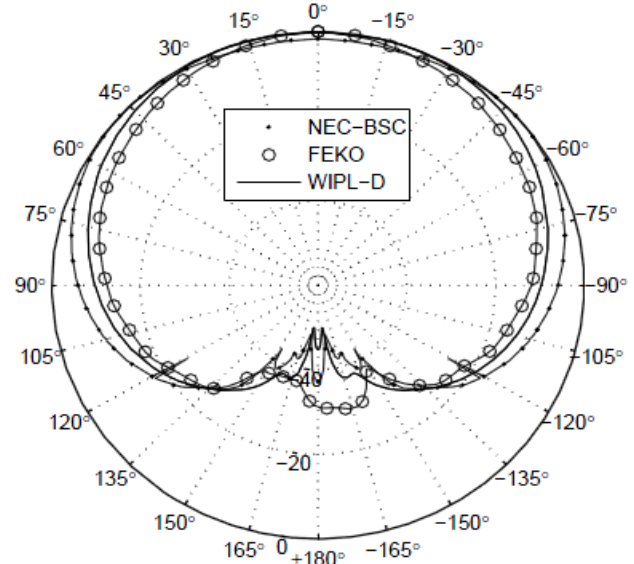


Fig. 6. Comparison of radiation patterns vs. azimuth angle ϕ , in the $\theta = 90^\circ$ plane for a 7-element $\lambda/2$ dipole array with central element excited and all others terminated in a 50Ω load $ka = 10$, $s/\lambda = 0.25$, $b/\lambda = 0.5$, $L/\lambda = 0.5$, $\alpha = 18.013^\circ$, and cylinder height is $H/\lambda = 10$.

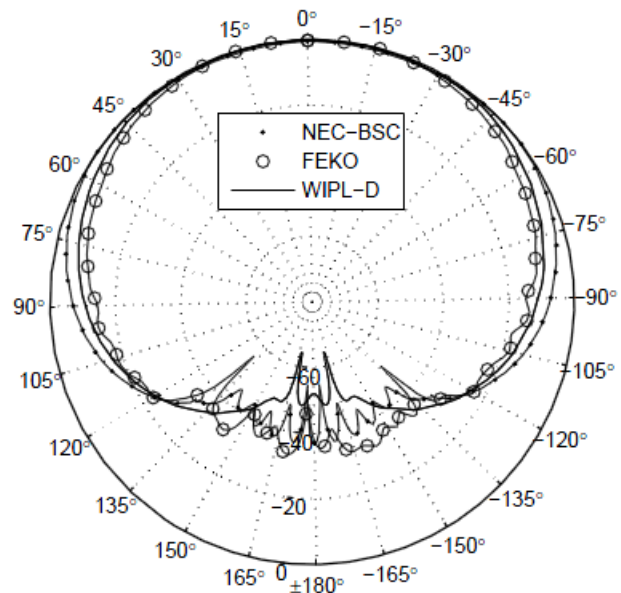


Fig. 7. Comparison of radiation patterns vs. azimuth angle ϕ , in the $\theta = 90^\circ$ plane for a 7-element $\lambda/2$ dipole array with central element excited and all others terminated in a 50Ω load $ka = 20$, $s/\lambda = 0.25$, $b/\lambda = 0.5$, $L/\lambda = 0.5$, $\alpha = 9.006^\circ$, and cylinder height is $H/\lambda = 10$.

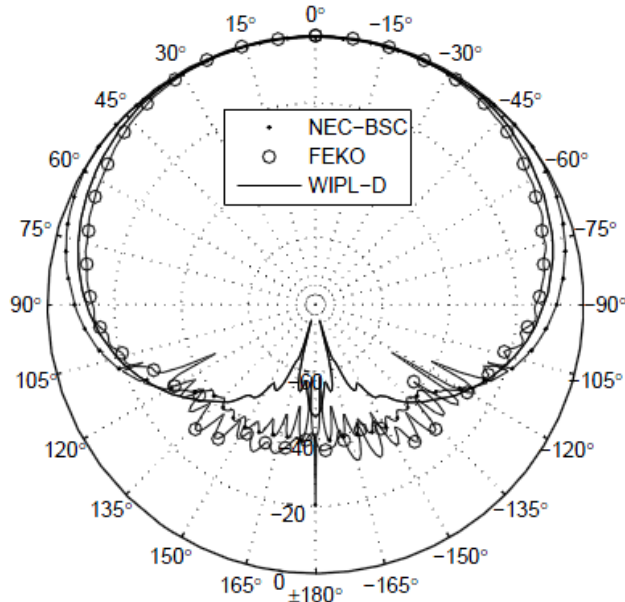


Fig. 8. Comparison of radiation patterns vs. azimuth angle ϕ , in the $\theta = 90^\circ$ plane for a 7-element $\lambda/2$ dipole array with central element excited and all others terminated in a 50Ω load $ka = 30$, $s/\lambda = 0.25$, $b/\lambda = 0.5$, $L/\lambda = 0.5$, $\alpha = 6.005^\circ$, and cylinder height is $H/\lambda = 10$.

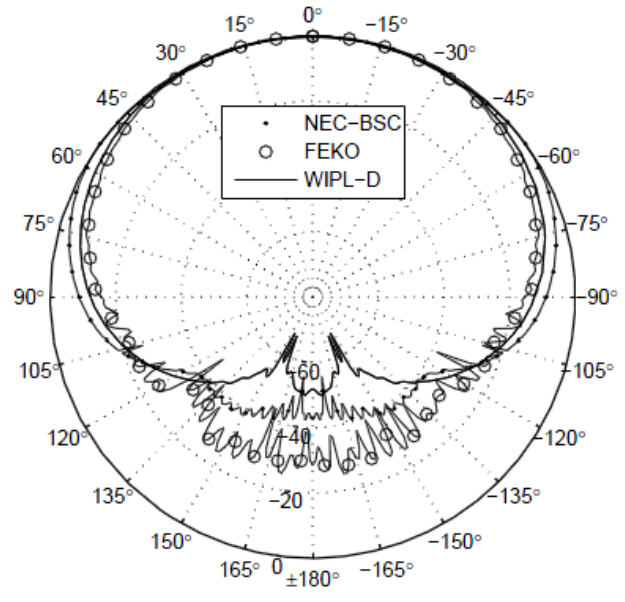


Fig. 10. Comparison of radiation patterns vs. azimuth angle ϕ , in the $\theta = 90^\circ$ plane for a 7-element $\lambda/2$ dipole array with central element excited and all others terminated in a 50Ω load $ka = 40$, $s/\lambda = 0.25$, $b/\lambda = 0.5$, $L/\lambda = 0.5$, $\alpha = 4.497^\circ$, and cylinder height is $H/\lambda = 10$.

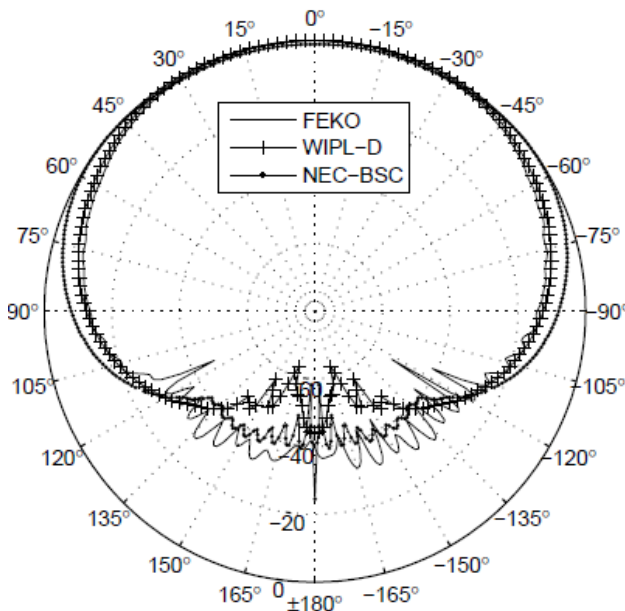


Fig. 9. All of the data is the same as in Fig. 8 above. For NECBSC results, the currents on the dipoles were approximated as that on the central segment of each dipole. The data here is taken from [15].

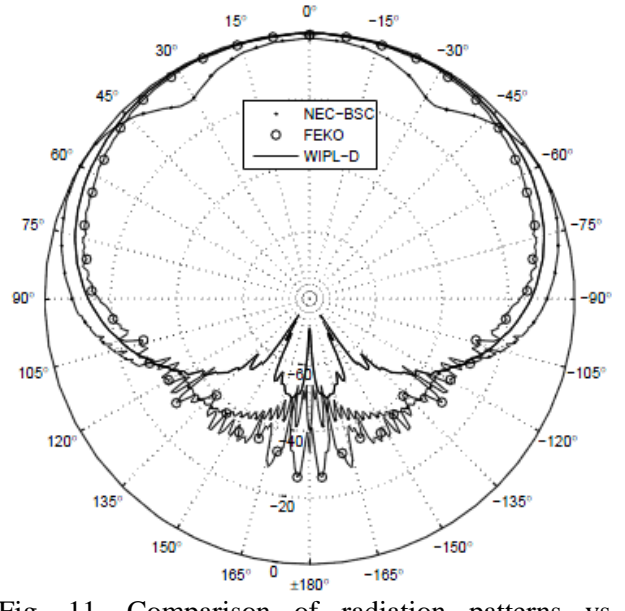


Fig. 11. Comparison of radiation patterns vs. azimuth angle ϕ , in the $\theta = 90^\circ$ plane for a 7-element $\lambda/2$ dipole array with central element excited and all others terminated in a 50Ω load $ka = 60$, $s/\lambda = 0.25$, $b/\lambda = 0.5$, $L/\lambda = 0.5$, $\alpha = 2.923^\circ$, and cylinder height is $H/\lambda = 10$.

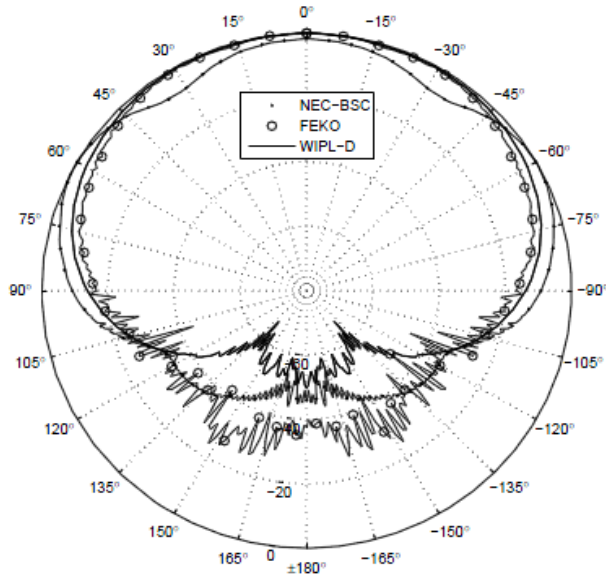


Fig. 12. Comparison of radiation patterns vs. azimuth angle ϕ , in the $\theta = 90^\circ$ plane for a 7-element $\lambda/2$ dipole array with central element excited and all others terminated in a 50Ω load $ka = 80$, $s/\lambda = 0.25$, $b/\lambda = 0.5$, $L/\lambda = 0.5$, $\alpha = 2.207^\circ$, and cylinder height is $H/\lambda = 10$.

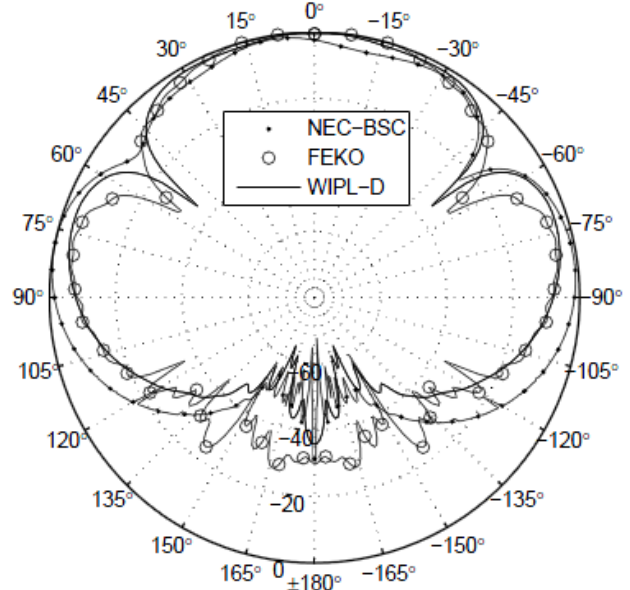


Fig. 14. Comparison of radiation patterns vs. azimuth angle ϕ , in the $\theta = 90^\circ$ plane for a 7-element $\lambda/2$ dipole array with central element excited and all others terminated in a 50Ω load $ka = 30$, $s/\lambda = 0.75$, $b/\lambda = 0.5$, $L/\lambda = 0.5$ and cylinder height is $H/\lambda = 10$.

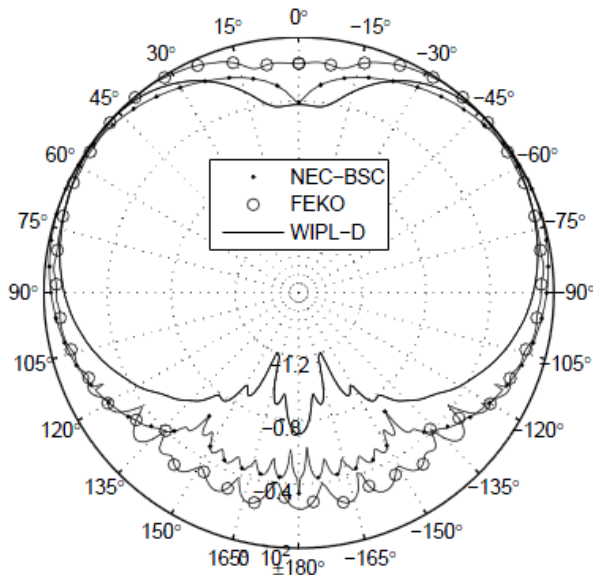


Fig. 13. Comparison of radiation patterns vs. azimuth angle ϕ , in the $\theta = 90^\circ$ plane for a 7-element $\lambda/2$ dipole array with central element excited and all others terminated in a 50Ω load $ka = 30$, $s/\lambda = 0.5$, $b/\lambda = 0.5$, $L/\lambda = 0.5$, and cylinder height is $H/\lambda = 10$.

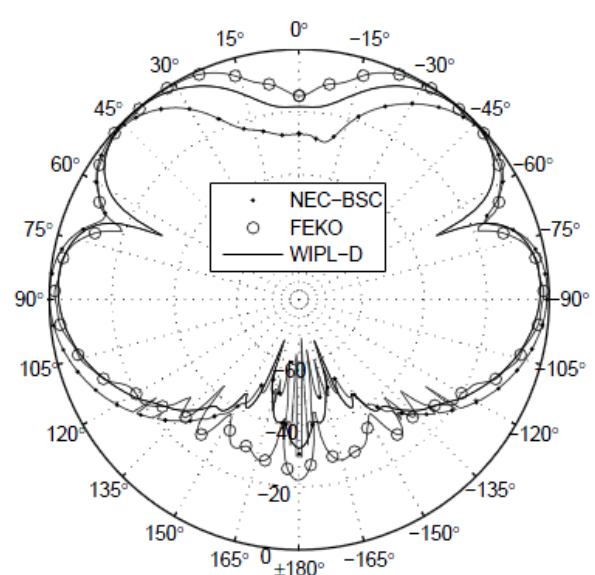


Fig. 15. Comparison of radiation patterns vs. azimuth angle ϕ , in the $\theta = 90^\circ$ plane for a 7-element $\lambda/2$ dipole array with central element excited and all others terminated in a 50Ω load $ka = 30$, $s/\lambda = 1.0$, $b/\lambda = 0.5$, $L/\lambda = 0.5$ and cylinder height is $H/\lambda = 10$.

IV. Summary and Conclusion

In this investigation a technique by which mutual coupling effects can be included while modeling a conformal dipole array via the high-frequency NECBSC code, has been developed by utilizing the output from the exact integral equation solver as contained in the commercially available FEKO code. The embedded element patterns for a seven element array were compared via FEKO, WIPL-D and NECBSC codes. The results showed that in the deep shadow region the disagreements were more pronounced for cylinders with electrically large radius of curvature. This is an interesting observation because NECBSC is expected to be more accurate as the cylinder size increased. Furthermore, it was found that the effect of the curvature on the element currents in the dipole array was insignificant beyond $ka \geq 50$. Thus, it was concluded that for electrically large conformal dipole arrays the solution to the dipole currents can be obtained to a reasonable degree of accuracy by solving an electrically smaller problem via the exact solvers such as FEKO or WIPL-D. The results of this investigation thus provide a computationally efficient strategy for determining radiation behavior of electrically large conformal arrays.

V. Acknowledgement

The authors remain grateful to Prof. Tapan K. Sarkar, EECS department, Syracuse University for the version of WIPL-D code used to generate the results, and, to Dr. C. J. Reddy EMS Software, Hampton, Virginia for technical support and use of FEKO software. The authors acknowledge the support from Dr. Kevin Z. Truman, Dean School of Computing and Engineering, UMKC, during the course of writing this paper. Finally, many useful technical discussions with Richard D. Swanson, Principal Engineer, Honeywell Federal Manufacturing and Technologies (FM & T), Kansas City, over the period of investigation of this project, helped improve the quality of the paper.

REFERENCES

- [1] L. Josefsson and P. Persson, *Conformal Array Antenna Theory and Design*. IEEE Wiley-Interscience, NY, USA, pp.101, 2006.
- [2] C. A. Balanis, *Antenna Theory: Analysis and Design* (3rd edition). John-Wiley & Sons, Inc., NY, 2005.
- [3] D. B. Davidson, *Computational Electromagnetics for RF and Microwave Engineering*. Cambridge University Press, NY, 2008 (digital reprint).
- [4] FEKO User's Manual (Suite # 5.3). EM Software and Systems, Norfolk, VA, USA, July 2007.
- [5] T. K. Sarkar, *WIPL-D User's Manual*, OHRN Enterprises, NY, USA; (private communication).
- [6] H. T. Chou, P. H. Pathak and M. Hsu, "Extended Uniform Geometrical Theory of Diffraction Solution for the Radiation by Antennas Located Close to an Arbitrary, Smooth, Perfectly Conducting, Convex Surface," *Radio Science*, vol. 32, no. 4, pp. 1297-1317, July-August 1997.
- [7] R. J. Marhefka and J. W. Silvestro, "Near Zone -Basic Scattering Code (User's Manual with Space Station Application)," technical report #716199-13, NASA, Hampton, VA, by the ElectroScience Laboratory, Ohio State University, Columbus, OH, USA, March 1989.
- [8] J. C. Herper, A. Hessel and B. Tomasic, "Element Pattern of an Axial Dipole in a Cylindrical Phased Array, Part II: Element Design and Experiments," *IEEE Trans. Antennas Propagat.*, vol. AP-33, pp. 273-278, March 1985.
- [9] F. G. Leppington, "Creeping Waves in the Shadow of an Elliptic Cylinder," *Jour. Inst. Math. Applics.* vol. 3, pp. 388402, 1967.
- [10] P. Hussar and R. Albus, "On the Asymptotic Behavior of Uniform GTD in the Shadow of a Smooth, Convex Surface," *IEEE Trans. Antennas. Propag.*, vol. 39, no. 12, pp. 1672-1680, December 1991.
- [11] R. Paknys, "On the Accuracy of the UTD for Scattering by a Cylinder," *IEEE Trans. Antennas. Propag.*, vol. 42, no. 5, pp. 757-760, May 1994.
- [12] S. D. Walker, "Surface Curvature Effects on the Scan Element Pattern of a Sector Electric-Dipole Array above a Cylindrical PEC Surface," FEKO International Student Competition, September 2008.
- [13] S. D. Walker and D. Chatterjee, "Studies on Development of Conformal Antennas and

Arrays,” final technical report #ECE-UMKC08HNYWL-TR01, Honeywell Federal Manufacturing and Technologies (FM & T), contract #224256, CSEE Dept., School of Computing and Engineering, UMKC, KC, MO, USA, September 2008.

- [14] S. D. Walker and D. Chatterjee, “Surface Curvature Effects on Element Characteristics on Large, Finite, Conformal Cylindrical Dipole Arrays,” *Proc. IEEE Intl. Symp. Antennas and Propagat.*, (4 pages), San Diego, USA, July 5-11, 2008.
- [15] S. D. Walker and D. Chatterjee, “Study of Exact and High-Frequency Code Solvers for Applications to a Conformal Cylindrical Dipole Array,” *Proceedings of the Annual Review of Progress in Applied Computational Electromagnetics*, (6 pages), Monterey, California. March 08-12, 2009.

Shaun D. Walker obtained bachelor’s degrees in Electrical and Computer Engineering (BSECE) and Computer Science (BSCS) from the Computer Science and Electrical Engineering Department at the University of Missouri-Kansas City (UMKC) in 2006, and is currently finishing his MSEE with the same department. His research interests are in analytical and numerical methods in electromagnetics for electrically large problems, conformal arrays and propagation in layered media. Shaun participated in the FEKO International Student Competition in 2008 and his report on conformal arrays received a special mention. In 2009 (June to August), Shaun worked as a ASEE-ONR student researcher at the US Naval Research Laboratory, Washington, DC on problems related to radiation from antennas embedded inside layered media. Shaun is simultaneously dual enrolled in the doctoral (PhD) degree program at UMKC.

Deb Chatterjee received BSETE, M.Tech, M.A.Sc and PhD degrees in 1981, ’83, ’92 and ’98, respectively. From 1983-1986 he worked with the Antenna Group at Hindustan Aeronautics Limited (HAL), Hyderabad, India. Since August 1999 he is with the Computer Science and Electrical Engineering (CSEE) department, University of Missouri Kansas City (UMKC), where he is now an associate professor. His research interests are in analytical and numerical techniques in electromagnetics, with an emphasis on high-frequency (asymptotic) applications, phased arrays and electromagnetic effects in biological systems. In 2009 (June to August) he was ASEE-ONR summer faculty fellow at the US Naval Research Laboratory, Washington, DC working on electromagnetic propagation problems in layered media. Dr. Chatterjee is a member of the IEEE Antennas and Propagation and Applied Computational Electromagnetics Societies, and reviewer for the *IEEE Transactions on Antennas and Propagation*, *IEEE Antennas and Wireless Propagation Letters*, *IEEE Antennas and Propagation Magazine*, *Applied Computational Electromagnetics Society Journal*, and *Radio Science*. He currently serves as an associate editor for the *International Journal on Antennas and Propagation* (Hindawi publications).